

Microstructural Brain Tissue Damage in Metabolic Syndrome

Michiel Sala,¹ Albert de Roos,¹
Annette van den Berg,¹
Irmhild Altmann-Schneider,^{1,2,3}
P. Eline Slagboom,^{3,4}
Rudi G. Westendorp,^{2,3}
Mark A. van Buchem,^{1,3}
Anton J.M. de Craen,^{2,3} and
Jeroen van der Grond^{1,3}

OBJECTIVE

We investigated the association between metabolic syndrome risk factors and brain tissue integrity, as assessed by magnetic resonance imaging.

RESEARCH DESIGN AND METHODS

From the Leiden Longevity Study, which is a community-based study of long-lived subjects, their offspring, and partners thereof, 130 subjects (61 men; mean age 66 years) were included. A metabolic syndrome score was computed by summing the individual number of components according to the Adult Treatment Panel III criteria. We performed linear and logistic regression analysis and used standardized β -values to assess the association between metabolic syndrome and brain macrostructure (brain volume and white matter lesion load, lacunar infarcts, and cerebral microbleeds) and microstructure (mean magnetization transfer ratio [MTR], MTR histogram peak height, fractional anisotropy, and mean diffusivity [MD]). Linear and stepwise regression analysis was performed to identify the individual contribution of one metabolic syndrome parameter adjusting for the four other parameters. Models were adjusted for age, sex, and relation to long-lived family.

RESULTS

Brain macrostructure was not associated with metabolic syndrome. In contrast, metabolic syndrome was associated with decreased gray ($\beta = -0.3$, $P = 0.001$) and white matter peak height ($\beta = -0.3$, $P = 0.002$) and increased gray matter MD ($\beta = 0.2$, $P = 0.01$, $P = 0.01$). Serum HDL cholesterol ($\beta = 0.22$, $P = 0.012$), triglycerides ($\beta = -0.25$, $P = 0.002$), BMI ($\beta = -0.2$, $P = 0.014$), and diastolic blood pressure ($\beta = -0.17$, $P = 0.047$, and $\beta = -0.23$, $P = 0.009$, for gray and white matter, respectively) were independent factors in these changes in brain microstructure.

CONCLUSIONS

In early manifest metabolic syndrome, brain tissue decline can be detected. Serum HDL cholesterol, triglycerides, BMI, and diastolic blood pressure were independent factors in brain tissue integrity.

Diabetes Care 2014;37:493–500 | DOI: 10.2337/dc13-1160

¹Department of Radiology, Leiden University Medical Center, Leiden, the Netherlands

²Department of Gerontology and Geriatrics, Leiden University Medical Center, Leiden, the Netherlands

³Netherlands Consortium for Healthy Ageing, Leiden, the Netherlands

⁴Department of Molecular Epidemiology, Leiden University Medical Center, Leiden, the Netherlands

Corresponding author: Michiel Sala, m.i.sala@lumc.nl.

Received 15 May 2013 and accepted 24 September 2013.

© 2014 by the American Diabetes Association. See <http://creativecommons.org/licenses/by-nc-nd/3.0/> for details.

Cardiovascular disease is considered the main long-term complication of metabolic syndrome and obesity-related disorders, although also multiple organs may be affected, including the brain (1). Considering brain damage, vascular risk factors associated with metabolic syndrome accelerate cerebral small vessel disease, which may result in white matter lesions, cerebral microbleeds, and brain atrophy, as detected by magnetic resonance imaging (MRI) (2,3). MRI studies of the brain have shown that early confluent and confluent white matter hyperintensities are related to vascular cognitive impairment (4). Moreover, white matter atrophy in obesity-related disorders like type 2 diabetes has been associated with progressive neurocognitive decline (5). Preceding macrostructural brain tissue damage, early microstructural changes may occur in the normal appearing brain tissue, which may play a role in the development of cognitive decline (4). However, the exact mechanism and histopathology of these brain tissue changes are still not fully defined.

Magnetization transfer imaging (MTI) and diffusion tensor imaging (DTI) are imaging techniques that are well suited to detect early microstructural changes in normal-appearing brain tissue in a number of disease states. Diffusion tensor imaging probes the direction and magnitude of water diffusion in the intracellular cytoplasm along the axons, whereas magnetization transfer imaging probes the protons bound to large molecules like the myelin lipids and proteins (4).

Recent studies demonstrated that microstructural brain tissue changes in association with metabolic and vascular risk factors using magnetization transfer and diffusion tensor imaging (6–8). However, evidence of metabolic syndrome as a risk factor per se is rather sparse (9). Moreover, it is unknown whether changes in microstructural brain tissue integrity in metabolic syndrome are present before imaging evidence of cerebral small vessel disease may become overt.

We hypothesized that clustering of metabolic syndrome risk factors increases the risk for microstructural

brain tissue decline in a dose-related fashion before imaging evidence of small vessel disease may become apparent. Therefore, we used a summary score for metabolic syndrome, as a categorical definition of metabolic syndrome may limit the power to detect an association (10). The purpose of this study was to investigate whether changes in brain microstructure are present in association with metabolic syndrome, independent of brain atrophy or imaging correlates of cerebral small vessel disease, as assessed by conventional structural MRI. Furthermore, we investigated the independent association between the individual metabolic syndrome components and brain tissue integrity, as assessed by magnetization transfer and diffusion tensor imaging.

RESEARCH DESIGN AND METHODS

Subjects were included from the Leiden Longevity Study, which has been described in more detail elsewhere (11). In short, 421 Dutch Caucasian families were enrolled in the study between 2002 and 2006 based on the following inclusion criteria: 1) there were at least two living siblings per family who fulfilled the age criteria and were willing to participate, 2) men had to be aged ≥ 89 years and women had to be aged ≥ 91 years, and 3) the sib pairs had to have the same parents. Additionally, offspring of these long-lived siblings were included, as they have a 35% lower mortality rate compared with the general population. Their partners, who share the same socioeconomic and geographical background, were enrolled as the age-matched control group (11). There were no selection criteria on health or demographic characteristics.

For the current study, subjects were recruited from the offspring of the long-lived siblings and their spouses. Inclusion criteria were complete data on metabolic syndrome criteria and all brain MRI imaging (structural, MTI, and DTI) data.

Subjects with diabetes were excluded. Subjects were regarded as having diabetes if they had nonfasted glucose levels > 11.0 mmol/L or used glucose-lowering agents.

The Medical Ethics Committee of the Leiden University Medical Center

approved the study, and written informed consent was obtained from all subjects according to the Declaration of Helsinki.

Metabolic Syndrome

According to the Adult Treatment Panel III criteria (12), metabolic syndrome risk factors in this study were defined as follows: 1) BMI > 25 kg/m², 2) decreased plasma HDL cholesterol levels (HDLc) (< 40 mg/dL [1.0 mmol/L] in males; < 50 mg/dL [1.3 mmol/L] in females), 3) increased plasma triglyceride levels (≥ 150 mg/dL [1.7 mmol/L]) or administration of lipid-lowering therapy, 4) elevated blood pressure or administration of antihypertensive medication (systolic pressure ≥ 130 mmHg or diastolic pressure ≥ 85 mmHg), and 5) increased fasting plasma glucose levels (≥ 100 mg/dL [5.6 mmol/L]) or treatment with glucose-lowering medication. We calculated a metabolic syndrome score by summing the number of factors, ranging from zero (no factors) to five (all metabolic syndrome factors). Presence of metabolic syndrome was defined as having three or more of any of the metabolic syndrome risk factors (12).

Measures of Cognitive Function

Cognitive testing in the Leiden Longevity Study has been described in more detail elsewhere (13). In short, memory function was evaluated with the 15-Picture Learning Test (15-PLT), and attention and processing speed were evaluated by using the Stroop test part 3 and the Digit Symbol Substitution Test (DSST). Outcome parameters for 15-PLT were the number of correct pictures after each trial (PLT-immediate) and after 20 min (PLT-delayed). For the Stroop test, the time needed to complete the test was defined as outcome parameter. Outcome parameter for the DSST was the number of correct digit-symbol combinations within 90 s.

MRI Acquisition

All imaging was performed on a whole-body magnetic resonance system operating at 3 Tesla field strength (Philips Medical Systems, Best, the Netherlands). Three-dimensional T1-weighted images were acquired with repetition time (TR) = 9.7 ms, echo time (TE) = 4.6 ms, flip angle (FA) = 8°, and

224 × 177 × 168 mm field of view (FOV), resulting in a nominal voxel size of 1.17 × 1.17 × 1.4 mm. Fluid-attenuated inversion recovery (FLAIR) images were acquired with TR = 11,000 ms, TE = 125 ms, FA = 90°, FOV = 220 × 176 × 137 mm, matrix size 320 × 240, and 25 transverse slices 5 mm thick. T2-weighted images were acquired with TR = 4,200 ms, TE = 80 ms, FA = 90°, FOV = 224 × 180 × 144 mm, matrix size 448 × 320, and 40 slices 3.6 mm thick. T2*-weighted images were acquired with TR = 45 ms, TE = 31 ms, FA = 13°, and FOV = 250 × 175 × 112 mm. Diffusion tensor images were acquired with TR = 9,592 ms, TE = 56 ms, FA = 90°, FOV = 220 × 220 × 128 mm, matrix size 112 × 110, 64 slices 2 mm thick, 32 measurement directions, and *b* value = 1,000. Magnetization transfer imaging was performed with TR = 100 ms, TE = 11 ms, FA = 9°, FOV = 224 × 180 × 144 mm, matrix size 224 × 169, and 20 slices 7 mm thick.

Image Processing and Analysis

For analysis of MRI scans, different tools of the FSL (Functional MRI of the Brain Software Library) software package were used (14,15). Gray and white matter volumes were calculated as previously described (16), and lacunar infarcts and cerebral microbleeds were evaluated as previously reported (17). White matter lesion volume in millimeters was automatically quantified by using a previously validated method (18). In short, after initial tissue segmentation (18), white matter masks generated by FSL were spatially transformed to FLAIR images by using the FLIRT tool (19). White matter hyperintensities were automatically identified from the mask by using a threshold of 3 SD above the mean FLAIR signal intensity, which was obtained from the cerebral periphery to limit skewing of the signal intensity distribution from hyperintense periventricular white matter voxels (18). The individual raw diffusion tensor images were preprocessed in order to create individual FA and mean diffusivity (MD) images using tools of FDT (FMRIB's Diffusion Toolbox) (20–22).

For creation of individual brain masks for cortical gray and white matter,

three-dimensional T1-weighted images were skull stripped (23) and subsequently segmented (24,25). Individual magnetization transfer ratio (MTR) maps were calculated voxel by voxel, and mean MTR and normalized peak height were calculated (26). For correction for possible partial volume effects, an eroded mask of the brain parenchyma and gray and white matter volume T1-weighter image segmentations was created by removing one voxel in plane for all mentioned volumes of interest (26).

Voxel-wise statistical analysis of white matter FA and MD was performed using Tract Based Spatial Statistics (27). First, FA images were brain extracted (28). All subjects' FA data were then aligned into a common space (29,30). Next, the mean FA image was created and thinned to create a mean FA skeleton, which represents the centers of all tracts common to the group. Each subject's aligned FA data were then projected onto this skeleton, and the resulting data were fed into voxel-wise cross-subject statistics. In the same manner, voxel-wise analysis of white matter MD data was performed.

We investigated the spatial distribution of changes in gray matter MTR on a voxel-wise basis. MTR maps were coregistered to the three-dimensional T1-weighted images and subsequently processed (31,32) with FSL tools (14). Next, voxel-wise statistics was carried out. Voxel-based analysis of DTI has not been performed since these data have been shown to depend highly on choice of normalization method, size of the smoothing kernel, and statistics and should therefore be interpreted with extreme caution (33).

Statistical Analysis

If not otherwise stated, data are presented as means (SD) (characteristics of the study population). Differences in subject demographics between offspring of long lived and their partners were calculated using independent-sample Mann-Whitney *U* test and Pearson χ^2 test.

Z scores were calculated for brain volume, white matter lesion volume, and MRI markers of brain microstructure. Accordingly, linear and

logistics regression analysis was performed to investigate associations between metabolic syndrome score, presence of metabolic syndrome (yes/no), and brain volume z score, MRI markers of cerebral small vessel disease (white matter lesion volume z score, lacunar infarcts, and cerebral microbleeds), and z scores for MRI markers of brain microstructure. Models were adjusted for age, sex, and descent (Leiden-longevity offspring or their partners).

To investigate to what extent associations between metabolic syndrome and changes in brain microstructure are mediated by the presence of cerebral microbleeds, we used an additional model that adjusted for the presence of cerebral microbleeds.

Linear and stepwise regression analyses were performed to identify which metabolic syndrome factors were independently associated with gray and white matter peak height z score and gray matter MD z score. In these analyses, continuous variables were used, and both systolic and diastolic blood pressure were included. Additional analyses adjusted for use of antihypertensive medication.

To estimate the association between metabolic syndrome and cognition (as assessed by 15-PLT, Stroop test, and DSST), we performed linear regression analysis using different models. Model 1 adjusted for age, sex, years of education, cardiovascular disease, and relation to descent (offspring of long lived or partner). Model 2 included model 1 and adjusted additionally for MRI markers of macrostructural brain damage. In addition, we also investigated whether MRI markers of brain microstructure were associated with cognition, adjusting for potential confounders as in model 1.

For statistical analyses, SPSS software for windows (version 20.0) was used. For voxel-wise statistical analyses, the FSL randomize tool was used to perform permutation-based nonparametric testing (*n* = 5,000 permutations) on the magnetization transfer data. Threshold-free cluster enhancement (34) was applied, which is generally more robust

and avoids the need for an arbitrary initial cluster-forming threshold (34). For correction for multiple comparisons across Montreal Neurological Institute 152 standard space, the statistical threshold was set at $P < 0.05$, Family-wise error corrected, which is a commonly used threshold in voxel wise analysis (35,36). Differences between subjects with and without metabolic syndrome were assessed adjusted for age, sex, and descent. For investigation of the association between metabolic syndrome score and MTR values, contrasts of interest were made for the metabolic syndrome score regressor. For metabolic syndrome (yes/no), the same model was used, though with contrast of interest made for the metabolic syndrome score regressor.

RESULTS

Subject characteristics are shown in Table 1. The study cohort consisted of 130 subjects ($n = 73$ offspring, $n = 57$

partners). Age, sex, history of disease, and prevalence of vascular risk and dichotomized metabolic syndrome factors (e.g., high HDLC yes/no) were similar between offspring of long lived and partners. Also, prevalence of metabolic syndrome (≥ 3 factors according to Adult Treatment Panel III criteria) was not different between the two groups. Mean fasted serum glucose was lower in the offspring group (mean \pm SEM serum glucose 4.95 ± 0.05 vs. 5.22 ± 0.08 mmol/L, $P = 0.03$). Clustering of metabolic syndrome components in the study cohort was as follows: in 31 (24%) subjects, no metabolic syndrome risk factors were present; in 56 (43%) subjects, one risk factor was present; in 25 (19%) subjects, two risk factors were present; in 14 (11%) subjects, three risk factors were present; in four (3%) subjects, four risk factors were present; and none of the study subjects had five metabolic syndrome risk factors.

Gray and white matter volume, white matter lesion volume, and prevalence of lacunar infarcts and cerebral microbleeds in association with metabolic syndrome score are shown in Table 2. There was no association between metabolic syndrome score and brain macrostructure (brain volume, MRI markers of cerebral small vessel disease). However, increasing metabolic syndrome score was associated with decreased gray ($\beta = -0.3$, $P = 0.001$) and white matter peak height ($\beta = -0.3$, $P = 0.0002$) and increased gray matter diffusivity ($\beta = 0.2$, $P = 0.01$).

We found no difference in brain macrostructure in subjects with metabolic syndrome (e.g., ≥ 3 risk factors) compared with subjects without the syndrome. However, subjects with the syndrome had lower gray and white matter peak height ($P = 0.02$ and $P = 0.03$, respectively) and increased gray matter MD ($P = 0.04$). Adjustment for the presence of cerebral microbleeds did not affect the observed associations between metabolic syndrome and MRI markers of brain microstructure.

Univariate and independent associations between the individual metabolic syndrome factors and brain MRI markers are shown in Table 3. Univariate analysis showed significant associations with gray and white matter peak height for HDLC, serum triglycerides, and BMI. Blood pressure was significantly associated with gray matter MD ($\beta = 0.19$, $P = 0.037$). Stepwise regression analysis showed that HDLC ($\beta = 0.22$, $P = 0.012$) and BMI ($\beta = -0.2$, $P = 0.014$) were independently associated with gray matter peak height. Serum triglycerides ($\beta = -0.25$, $P = 0.002$) and BMI ($\beta = -0.16$, $P = 0.047$) were associated with white matter peak height. Higher systolic and diastolic blood pressure showed a trend toward increased MD, although nonsignificant ($P = 0.06$ and $P = 0.06$, respectively). However, after adjustment for use of antihypertensive medication, diastolic blood pressure was significantly associated with gray matter ($\beta = -0.17$, $P = 0.047$) and white matter ($\beta = -0.23$, $P = 0.009$) peak height.

Table 1—Characteristics of the study cohort

Characteristics	Subjects ($n = 130$)
<i>n</i>	130
Men, <i>n</i> (%)	61 (47)
Age in years, mean (SD)	66.2 (6.7)
Offspring of long lived (%)	57 (44)
Current smoking, <i>n</i> (%)	11 (8)
History of disease, <i>n</i> (%)	
COPD	7 (5)
Stroke	1 (1)
Myocardial infarct	1 (1)
Metabolic syndrome-related characteristics, mean (SD)	
HDLC (mmol/L)	1.5 (0.6)
Triglyceride (mmol/L)	1.4 (0.6)
Fasted glucose (mmol/L)	5.1 (0.6)
Weight (kg)	79.0 (13.6)
Height (cm)	172.6 (8.2)
BMI (kg/m ²)	26 (4)
Systolic blood pressure (mmHg)	139 (19)
Diastolic blood pressure (mmHg)	83 (10)
Dichotomized vascular risk factors, <i>n</i> (%)	
Low HDLC	23 (18)
High triglycerides	30 (14)
High glucose	9 (7)
High BMI	18 (14)
High blood pressure	84 (65)

Low HDLC: decreased plasma HDLC levels <1.0 mmol/L in males and <1.3 mmol/L in females; high triglycerides: increased plasma triglyceride levels >1.7 mmol/L or administration of lipid-lowering therapy; high glucose: increased fasting plasma glucose levels >5.6 mmol/L or treatment with glucose-lowering medication; high BMI: >25 kg/m²; high blood pressure: elevated blood pressure, systolic pressure ≥ 130 mmHg, diastolic pressure ≥ 85 mmHg, or administration of antihypertensive medication. Age in years = at MRI examination. COPD, chronic obstructive pulmonary disease; fasted glucose, fasting plasma glucose levels; triglycerides, plasma triglyceride levels.

Table 2—Association among brain volume, imaging characteristics of small-vessel disease and microstructural brain tissue integrity, and metabolic syndrome score

	Metabolic syndrome score					β /OR (95% CI)	<i>P</i>
	0	1	2	3	4		
<i>n</i>	31	56	25	14	4		
Brain volume (cm ³) ^a							
Gray matter	546 (7)	546 (5)	538 (8)	525 (8)	518 (2)	−0.1 (−0.2 to 0.1)	0.19
White matter	538 (10)	548 (7)	551 (1)	512 (1)	528 (4)	−0.06 (−0.2 to 0.1)	0.44
White matter lesion volume (mL)	1.2 (0.3)	2.6 (0.8)	2.6 (1.5)	2.6 (1.8)	0.09 (0.05)	−0.01 (−0.2 to 0.1)	0.71
Lacunar infarcts, <i>n</i> (%)	0 (0)	2 (4)	2 (8)	0 (0)	1 (25)	1.8 (0.8–4.2)	0.19
Cerebral microbleeds, <i>n</i> (%)	3 (10)	5 (9)	5 (20)	1 (7)	0 (0)	0.9 (0.5–1.8)	0.84
Mean MTR (value $\times 10^3$)							
Gray matter	337 (1)	333 (1)	332 (2)	330 (3)	329 (5)	−0.2 (−0.3 to 0.01)	0.071
White matter	397 (1)	393 (1)	394 (2)	396 (3)	393 (5)	0.01 (−0.2 to 0.2)	0.94
Normalized peak height (pixel count $\times 10^{-3}$)							
Gray matter	82 (2)	74 (2)	72 (3)	68 (3)	67 (3)	−0.3 (−0.4 to −0.1)	0.001
White matter	133 (3)	117 (3)	108 (5)	107 (6)	103 (11)	−0.3 (−0.4 to −0.1)	0.0002
Fractional anisotropy (value $\times 10^3$)							
Gray matter	195 (2)	198 (9)	198 (2)	194 (2)	200 (9)	0.04 (−0.1 to 0.2)	0.67
White matter	325 (2)	323 (2)	318 (3)	323 (4)	327 (4)	−0.04 (−0.2 to 0.1)	0.66
MD (mm ² /s $\times 10^6$)							
Gray matter	1,103 (5)	1,126 (8)	1,135 (11)	1,138 (17)	1,191 (21)	0.2 (0.04–0.3)	0.01
White matter	890 (4)	912 (6)	923 (8)	908 (10)	941 (12)	0.2 (−0.00 to 0.3)	0.06

Values are means (SE) unless otherwise indicated. Results are from logistic regression analysis for the prevalence of lacunar infarcts and cerebral microbleeds; odds ratios (95% CI) are shown. Multiple regression analysis was performed for all other variables; β (95% CI) represents the change in *z* score for structural brain MRI markers per SD increase in metabolic syndrome score. All analyses were performed correcting for age, sex, and descent. Metabolic syndrome score: individual prevalence of metabolic syndrome risk factors, e.g., score = 1, 1 risk factor present; score = 2, 2 risk factors present; and so on. ^aUnnormalized brain volume; corresponding *P* values are shown for analysis using individual brain volume normalized for head size.

Voxel-wise analysis of cortical gray matter MTR showed that changes were diffuse and symmetrical in both hemispheres, in association with increasing metabolic syndrome score (Fig. 1). Voxel-wise statistical analysis of white matter FA or MD showed no significant changes in association with metabolic syndrome.

We did not find any significant associations between metabolic syndrome (score and metabolic syndrome yes/no) and cognition. Also, none of the MRI markers for brain microstructure (MTR, peak height, FA, MD) were associated with cognitive function.

CONCLUSIONS

Our data show that clustering of risk factors in metabolic syndrome is associated with evidence of microstructural damage in the gray and white matter as indicated by decreased MTR peak height and increased MD. In contrast, we did not find evidence of macrostructural brain damage. Stepwise regression analysis showed

that HDLC, serum triglycerides, and BMI were independently associated with gray and white matter peak height. After adjustment for use of antihypertensive medication, diastolic blood pressure was also independently associated with gray and white matter peak height. Finally, voxel-wise analysis showed that subtle MTR changes do not occur in preferential brain regions.

Our data show that subjects with higher metabolic syndrome score neither demonstrate brain atrophy nor show increasing white matter volume or prevalence of lacunar infarcts and cerebral microbleeds. Previous studies report increasing white matter lesion burden and silent brain infarctions and increased brain atrophy in patients with type 2 diabetes (5) and hypertension (37). Cerebral small vessel disease can be regarded as an active process in which patients may be more susceptible to accelerated brain atrophy (2). Inclusion bias may be the underlying factor in the discrepancy between previous reports and our observed brain macrostructure in association with

metabolic syndrome. In the current study, all subjects were recruited from the Leiden Longevity Study (11), which is a community-based study comprising a relatively healthy cohort. Our data indicate that in subjects with asymptomatic or preclinical metabolic syndrome, changes in brain microstructure can be detected before larger visible neurodegenerative changes occur.

In one recent study, increased white matter MD without changes in FA in hypertensive patients was found (38). Other studies showed decreased white matter FA in type 1 diabetes (39) and metabolic syndrome (7,8). While FA reflects the coherence of highly structured tissue, e.g., white matter bundles, MD broadly reflects extracellular fluid accumulation. In our study, metabolic syndrome score was positively correlated with gray matter MD, but not with gray matter FA or white matter MD or FA. One possible explanation for the observed increase in gray matter MD with preserved FA is that, due to blood-brain barrier damage,

Table 3—Association between individual metabolic syndrome components and imaging characteristics for microstructural brain tissue integrity

	Gray matter peak height		White matter peak height		Gray matter MD	
	β (SE)	<i>P</i>	β (SE)	<i>P</i>	β (SE)	<i>P</i>
Univariate associations						
Glucose	−0.12 (0.09)	0.17	−0.04 (0.09)	0.66	0.093 (0.09)	0.3
HDLC	0.36 (0.1)	0.007	0.33 (0.1)	0.013	−0.019 (0.1)	0.88
Triglycerides	−0.21 (0.09)	0.018	−0.26 (0.09)	0.003	0.0001 (0.0)	0.99
BMI	−0.19 (0.09)	0.021	−0.19 (0.09)	0.031	0.13 (0.08)	0.12
Blood pressure	−0.14 (0.09)	0.16	−0.17 (0.09)	0.073	0.19 (0.09)	0.037
Model 1						
Glucose	−0.08	0.36	0.05	0.58	0.1	0.27
HDLC	0.22 (0.07)	0.012	0.12	0.18	−0.14	0.13
Triglycerides	−0.13	0.2	−0.25 (0.08)	0.002	0.024	0.79
BMI	−0.2 (0.08)	0.014	−0.16 (0.08)	0.047	0.16	0.08
Systolic RR	−0.13	0.15	−0.13	0.14	0.17	0.06
Diastolic RR	−0.16	0.08	−0.13	0.15	0.18	0.06
Model 2						
Glucose	−0.06	0.52	0.001	0.99	0.064	0.51
HDLC	0.21 (0.08)	0.026	0.27 (0.08)	0.002	−0.15	0.13
Triglycerides	−0.11	0.3	−0.17	0.073	0.034	0.73
BMI	−0.2 (0.09)	0.023	−0.15	0.12	0.065	0.51
Systolic RR	−0.06	0.57	−0.008	0.94	0.13	0.18
Diastolic RR	−0.17 (0.09)	0.047	−0.23 (0.09)	0.009	0.12	0.22

Univariate associations are from linear regression analysis, correcting for age, sex, and descent. Stepwise regression included the individual metabolic syndrome risk factors and age, sex, and descent (model 1) and, additionally, use of antihypertensive medications (model 2). The standardized β -coefficient (per increase in SD) with SE, or partial correlation, and corresponding *P* values are shown. Glucose, fasting plasma glucose levels; RR, respiratory rate.

early extracellular fluid accumulation appears before gray matter microstructural coherence, as assessed by FA, is affected.

One recent study showed modulatory effects of vascular risk factors on MTR histogram analysis: peak position shifted toward lower MTR values in

association with hypertension. Also, MTR peak height was lower in association with increasing HbA_{1c} (6). In our study, metabolic syndrome was

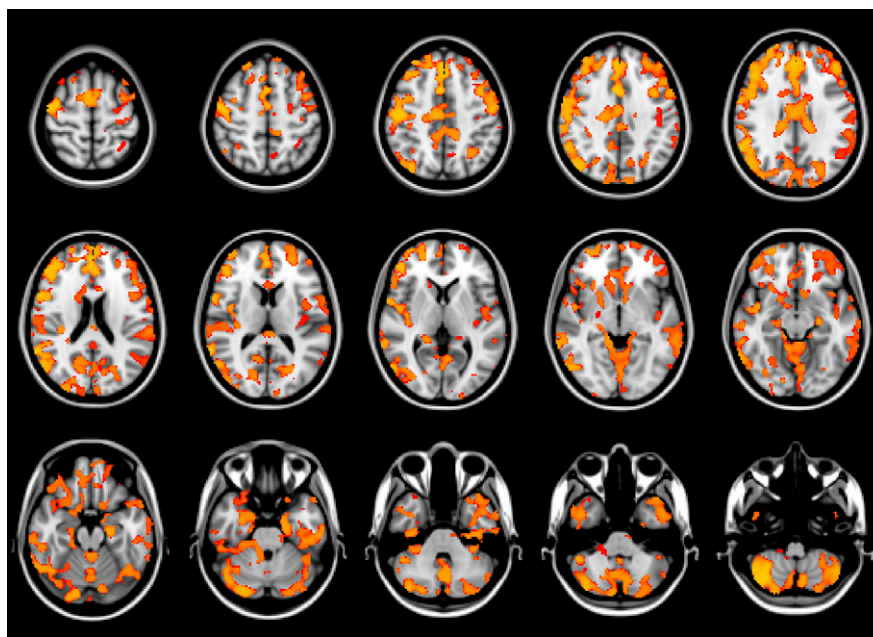


Figure 1—Voxel-based analysis of changes in cortical gray matter MTR associated with increasing metabolic syndrome score. Figure 1 shows results from the voxel-wise analysis of changes in cortical gray matter MTR in all subjects using FSL-VBM. Results are projected on the MNI152 space T1-weighted image provided by FSL. Areas showing statistically significant decline of gray matter MTR in association with a stepwise increase in metabolic syndrome risk factors (metabolic syndrome score) are highlighted in orange (*P* < 0.05, corrected). Statistical analysis was adjusted for sex, age, and descent (offspring of long lived or partner).

associated with lower gray and white matter MTR peak height. Lower peak height is thought to reflect an increase of tissue with low MTR values and thus to inversely reflect the burden of disease in patients (40). In addition, we found mean MTR values to be preserved. These findings potentially reflect brain tissue loss rather than demyelination or global microstructural changes (6). However, the exact biological nature of these measures is still not fully understood.

We found that gray and white matter peak heights were lower in subjects with low serum HDLC, high serum triglycerides, and high BMI. High blood pressure was associated with increased gray matter MD. However, owing to the selection for metabolic syndrome these are interrelated risk factors (12) in the study population. Nevertheless, stepwise regression analysis showed that HDLC, triglycerides, and BMI were independently associated with gray and white matter peak heights.

Previous studies have found associations between blood pressure and white matter lesions. However, results have been inconsistent regarding the relative importance of systolic and diastolic blood pressure (41,42). We found that, after adjustment for use of antihypertensive medication, diastolic but not systolic blood pressure was independently associated with gray and white matter peak height. Considering white matter damage, differences in underlying mechanisms may explain our observed results. Large artery atherosclerosis and arterial stiffness lead to elevated systolic blood pressure, whereas diastolic blood pressure and mean arterial pressure are more dependent on peripheral vascular resistance that may reflect small-vessel disease (42,43). By using voxel-based morphometry analysis, one recent study reported gray matter atrophy in frontal and temporal regions and different subcortical regions in mild cognitive impairment patients with first-ever lacunar infarction (44). These findings are consistent with functional neuroimaging data and provide evidence that beyond the area of infarction, remote effects of

subcortical damage may occur (45). By using voxel-wise analysis of MTR changes associated with metabolic syndrome, we found a diffuse, widespread, and symmetrical decrease in gray matter MTR in both hemispheres. Our results may be explained if these diffuse changes represent very subtle overall microstructural brain tissue damage providing a “setup” or increased vulnerability and, hence, a first step toward brain damage before actual focal ischemic lesions occur.

One recent study showed an anterior-posterior gradient of decrease in white matter FA in association with metabolic syndrome (7). In contrast, by using voxel-wise statistical analysis, we found no significant changes in white matter FA or MD in association with the syndrome. Also, we found no overt brain damage in association with metabolic syndrome. One potential explanation is that our study cohort comprised relatively healthy subjects. On the other hand, lack of statistical power to detect an association may have been a factor and should therefore be considered.

Metabolic syndrome has been associated with cognitive dysfunction (9). We did not find any significant associations between the syndrome, MRI markers of brain tissue integrity, and cognition, which may be explained by the relatively low age of our study subjects. An alternative explanation may be that subtle neuropathology has been shown to develop years before onset of clinical symptoms (46).

In conclusion, we found microstructural brain tissue decline in association with metabolic syndrome in middle-aged to elderly community-dwelling subjects. Serum HDL cholesterol, triglycerides, BMI, and diastolic blood pressure were independent factors. The observed diffuse and subtle changes in gray matter microstructure may represent an overall setup for brain damage preceding actual focal ischemic lesions, brain atrophy, and finally cognitive impairment. Future longitudinal studies should determine whether these changes evolve in more pronounced structural deterioration or cognitive decline. Our findings underline the

importance for early and comprehensive intervention and subsequent potential health gain in metabolic syndrome.

Funding. Funding was provided by Switchbox (FP7, Health-F2-2010-259772 [www.switchbox-online.eu]).

Duality of Interest. No potential conflicts of interest relevant to this article were reported.

Author Contributions. M.S. and I.A.-S. enrolled study subjects, gathered data, contributed to and edited the report, and approved the report before submission. A.d.R., P.E.S., and M.A.v.B. provided support on data analysis and interpretation, contributed to and edited the report, and approved the report before submission. A.v.d.B. analyzed and interpreted data, contributed to and edited the report, and approved the report before submission. R.G.W. and A.J.M.d.C. conceived the study and its initial design, contributed to and edited the report, and approved the report before submission. J.v.d.G. conceived the study and its original design; enrolled study subjects; gathered, analyzed, and interpreted data; contributed to and edited the report; and approved the report before submission. J.v.d.G. is the guarantor of this work and, as such, had full access to all the data in the study and takes responsibility for the integrity of the data and the accuracy of the data analysis.

References

- van der Meer RW, Lamb HJ, Smit JW, de Roos A. MR imaging evaluation of cardiovascular risk in metabolic syndrome. *Radiology* 2012;264:21–37
- Kloppenborg RP, Nederkoorn PJ, Grool AM, et al.; SMART Study Group. Cerebral small-vessel disease and progression of brain atrophy: the SMART-MR study. *Neurology* 2012;79:2029–2036
- Thompson CS, Hakim AM. Living beyond our physiological means: small vessel disease of the brain is an expression of a systemic failure in arteriolar function: a unifying hypothesis. *Stroke* 2009;40:e322–e330
- Seiler S, Cavalieri M, Schmidt R. Vascular cognitive impairment - an ill-defined concept with the need to define its vascular component. *J Neurol Sci* 2012;322:11–16
- van Elderen SG, de Roos A, de Craen AJ, et al. Progression of brain atrophy and cognitive decline in diabetes mellitus: a 3-year follow-up. *Neurology* 2010;75:997–1002
- Ropele S, Enzinger C, Söllinger M, et al. The impact of sex and vascular risk factors on brain tissue changes with aging: magnetization transfer imaging results of the Austrian stroke prevention study. *AJNR Am J Neuroradiol* 2010;31:1297–1301

7. Segura B, Jurado MA, Freixenet N, Falcón C, Junqué C, Arboix A. Microstructural white matter changes in metabolic syndrome: a diffusion tensor imaging study. *Neurology* 2009;73:438–444
8. Shimoji K, Abe O, Uka T, et al. White matter alteration in metabolic syndrome: diffusion tensor analysis. *Diabetes Care* 2013;36:696–700
9. Yates KF, Sweat V, Yau PL, Turchiano MM, Convit A. Impact of metabolic syndrome on cognition and brain: a selected review of the literature. *Arterioscler Thromb Vasc Biol* 2012;32:2060–2067
10. Franks PW, Ekelund U, Brage S, Wong MY, Wareham NJ. Does the association of habitual physical activity with the metabolic syndrome differ by level of cardiorespiratory fitness? *Diabetes Care* 2004;27:1187–1193
11. Schoenmaker M, de Craen AJ, de Meijer PH, et al. Evidence of genetic enrichment for exceptional survival using a family approach: the Leiden Longevity Study. *Eur J Hum Genet* 2006;14:79–84
12. Grundy SM, Cleeman JI, Daniels SR, et al.; American Heart Association; National Heart, Lung, and Blood Institute. Diagnosis and management of the metabolic syndrome: an American Heart Association/ National Heart, Lung, and Blood Institute Scientific Statement. *Circulation* 2005;112:2735–2752
13. Stijntjes M, de Craen AJ, van Heemst D, et al. Familial longevity is marked by better cognitive performance at middle age: the Leiden Longevity Study. *PLoS ONE* 2013;8:e57962
14. Smith SM, Jenkinson M, Woolrich MW, et al. Advances in functional and structural MR image analysis and implementation as FSL. *Neuroimage* 2004;23(Suppl. 1):S208–S219
15. Woolrich MW, Jbabdi S, Patenaude B, et al. Bayesian analysis of neuroimaging data in FSL. *Neuroimage* 2009;45(Suppl.):S173–S186
16. Altmann-Schneider I, de Craen AJ, Slagboom PE, et al. Brain tissue volumes in familial longevity: the Leiden Longevity Study. *Aging Cell* 2012;11:933–939
17. Altmann-Schneider I, van der Grond J, Slagboom PE, et al. Lower susceptibility to cerebral small vessel disease in human familial longevity: the Leiden Longevity Study. *Stroke* 2013;44:9–14
18. King KS, Chen KX, Hulsey KM, et al. White matter hyperintensities: use of aortic arch pulse wave velocity to predict volume independent of other cardiovascular risk factors. *Radiology* 2013;267:709–717
19. Jenkinson M, Smith S. A global optimisation method for robust affine registration of brain images. *Med Image Anal* 2001;5:143–156
20. Behrens TE, Woolrich MW, Jenkinson M, et al. Characterization and propagation of uncertainty in diffusion-weighted MR imaging. *Magn Reson Med* 2003;50:1077–1088
21. Behrens TE, Johansen-Berg H, Woolrich MW, et al. Non-invasive mapping of connections between human thalamus and cortex using diffusion imaging. *Nat Neurosci* 2003;6:750–757
22. Behrens TE, Berg HJ, Jbabdi S, Rushworth MF, Woolrich MW. Probabilistic diffusion tractography with multiple fibre orientations: What can we gain? *Neuroimage* 2007;34:144–155
23. Smith SM, Zhang Y, Jenkinson M, et al. Accurate, robust, and automated longitudinal and cross-sectional brain change analysis. *Neuroimage* 2002;17:479–489
24. Patenaude B, Smith SM, Kennedy DN, Jenkinson M. A Bayesian model of shape and appearance for subcortical brain segmentation. *Neuroimage* 2011;56:907–922
25. Zhang Y, Brady M, Smith S. Segmentation of brain MR images through a hidden Markov random field model and the expectation-maximization algorithm. *IEEE Trans Med Imaging* 2001;20:45–57
26. van den Bogaard SJ, Dumas EM, Milles J, et al. Magnetization transfer imaging in premanifest and manifest Huntington disease. *AJNR Am J Neuroradiol* 2012;33:884–889
27. Smith SM, Jenkinson M, Johansen-Berg H, et al. Tract-based spatial statistics: voxelwise analysis of multi-subject diffusion data. *Neuroimage* 2006;31:1487–1505
28. Smith SM. Fast robust automated brain extraction. *Hum Brain Mapp* 2002;17:143–155
29. Andersson JRL, Jenkinson M, Smith S. *Non-Linear Registration, aka Spatial Normalisation*. FMRIB Tech. Rep. TR07JA2, 1-1-2007
30. Andersson JRL, Jenkinson M, Smith S. *Non-Linear Optimisation*. FMRIB Tech. Rep. TR07JA1, 1-1-2007
31. Ashburner J, Friston KJ. Voxel-based morphometry—the methods. *Neuroimage* 2000;11:805–821
32. Good CD, Johnsrude IS, Ashburner J, Henson RN, Friston KJ, Frackowiak RS. A voxel-based morphometric study of ageing in 465 normal adult human brains. *Neuroimage* 2001;14:21–36
33. Jones DK, Cercignani M. Twenty-five pitfalls in the analysis of diffusion MRI data. *NMR Biomed* 2010;23:803–820
34. Smith SM, Nichols TE. Threshold-free cluster enhancement: addressing problems of smoothing, threshold dependence and localisation in cluster inference. *Neuroimage* 2009;44:83–98
35. Manninen O, Koskenkorva P, Lehtimäki KK, et al. White Matter Degeneration with Unverricht-Lundborg Progressive Myoclonus Epilepsy: A Translational Diffusion-Tensor Imaging Study in Patients and Cystatin B-Deficient Mice. *Radiology* 2013;269:232–239
36. Roosendaal SD, Schoonheim MM, Hulst HE, et al. Resting state networks change in clinically isolated syndrome. *Brain* 2010;133:1612–1621
37. Manolio TA, Olson J, Longstreth WT. Hypertension and cognitive function: pathophysiologic effects of hypertension on the brain. *Curr Hypertens Rep* 2003;5:255–261
38. Gons RA, de Laat KF, van Norden AG, et al. Hypertension and cerebral diffusion tensor imaging in small vessel disease. *Stroke* 2010;41:2801–2806
39. Kodl CT, Franc DT, Rao JP, et al. Diffusion tensor imaging identifies deficits in white matter microstructure in subjects with type 1 diabetes that correlate with reduced neurocognitive function. *Diabetes* 2008;57:3083–3089
40. van Buchem MA, Grossman RI, Armstrong C, et al. Correlation of volumetric magnetization transfer imaging with clinical data in MS. *Neurology* 1998;50:1609–1617
41. Gottesman RF, Coresh J, Catellier DJ, et al. Blood pressure and white-matter disease progression in a biethnic cohort: Atherosclerosis Risk in Communities (ARIC) study. *Stroke* 2010;41:3–8
42. Marcus J, Gardener H, Rundek T, et al. Baseline and longitudinal increases in diastolic blood pressure are associated with greater white matter hyperintensity volume: the northern Manhattan study. *Stroke* 2011;42:2639–2641
43. Guo X, Pantoni L, Simoni M, et al. Blood pressure components and changes in relation to white matter lesions: a 32-year prospective population study. *Hypertension* 2009;54:57–62
44. Grau-Olivares M, Arboix A, Junqué C, Arenaza-Urquijo EM, Rovira M, Bartrés-Faz D. Progressive gray matter atrophy in lacunar patients with vascular mild cognitive impairment. *Cerebrovasc Dis* 2010;30:157–166
45. Duering M, Righart R, Csanadi E, et al. Incident subcortical infarcts induce focal thinning in connected cortical regions. *Neurology* 2012;79:2025–2028
46. Jokinen H, Schmidt R, Ropele S, et al.; LADIS Study Group. Diffusion changes predict cognitive and functional outcome: the LADIS study. *Ann Neurol* 2013;73:576–583